BJR

https://doi.org/10.1259/bjr.20220238

Received: 28 February 2022 | Revised: 20 October 2022 | Accepted: 20 November 2022 | Published online: 04 January 2023

Cite this article as:
Shu X, Liu Y, Qiao X, Ai G, Liu L, Liao J, et al. Radiomic-based machine learning model for the accurate prediction of prostate cancer risk stratification. *Br J Radiol* (2023) 10.1259/bjr.20220238.

FULL PAPER

Radiomic-based machine learning model for the accurate prediction of prostate cancer risk stratification

[1]XIN SHU, MD, [1]YUNFAN LIU, MD, [1]XIAOFENG QIAO, MD, [1]GUANGYONG AI, MD, [2]LI LIU, PhD, [2]JUN LIAO, PhD, [2]ZHENGQIAO DENG, MD and [1]XIAOJING HE, PhD

[1]Department of Radiology, The Second Affiliated Hospital of Chongqing Medical University, Chongqing, China
[2]College of Big Data & Software Engineering, Chongqing University, Chongqing, China

Address correspondence to: Xiaojing He
E-mail: *he_xiaojing@hospital.cqmu.edu.cn*

Xin Shu and Yunfan Liu have contributed equally to this study and should be considered as co-first authors.

Objectives: To precisely predict prostate cancer (PCa) risk stratification, we constructed a machine learning (ML) model based on magnetic resonance imaging (MRI) radiomic features.
Methods: Between August 2016 and May 2021, patients with histologically proven PCa who underwent preoperative MRI and prostate-specific antigen screening were included. The patients were grouped into different risk categories as defined by the European Association of Urology-European Association of Nuclear Medicine-European Society for Radiotherapy and Oncology-European Society of Urogenital Radiology-International Society of Geriatric Oncology guidelines. Using Artificial Intelligence Kit software, PCa regions of interest were delineated and radiomic features were extracted. Subsequently, predictable models were built by utilising five traditional ML approaches: support vector machine, logistic regression, gradient boosting decision tree, k-nearest neighbour and random forest (RF) classifiers. The classification capacity of the developed models was assessed by area under the receiver operating characteristic curve (AUC) analysis.
Results: A total of 213 patients were enrolled, including 16 low-risk, 65 intermediate-risk, and 132 high-risk PCa patients. The risk stratification of PCa could be revealed by MRI radiomic features, and second-order features accounted for most of the selected features. Among the five established ML models, the RF model showed the best overall predictive performance (AUC = 0.87). After further analysis of the subgroups based on the RF model, the prediction of the high-risk group was the best (AUC = 0.89).
Conclusion: This study demonstrated that the MR radiomics-based ML method could be a promising tool for predicting PCa risk stratification precisely.
Advances in knowledge: The ML models have valuable prospect for accurate PCa risk assessment, which might contribute to customize treatment and surveillance strategies.

INTRODUCTION

Prostate cancer (PCa) is the most prevalent malignant neoplasm of the male genital system.[1] In 2021, the American Cancer Society (ACS) estimated 248,530 new PCa cases (13.1% of all new cancer cases) and 34,130 PCa-related deaths in the United States, imposing a substantial socioeconomic burden.[2] The detection rate of PCa is now increasing owing to the screening of prostate-specific antigen (PSA), digital rectal examination and advances in medical imaging, which leads to a reduction in advanced disease and specific mortality from PCa but also results in overdiagnosis and resultant overtreatment.[3,4] In a European randomised study of screening for PCa, which tested 61,404 men, no cancer was found in 76% of the prostate biopsies conducted for an elevated PSA.[5] Of those with a positive biopsy, an estimated 20–50% represent overdiagnosis.[6] It is acknowledged that not all patients with PCa should receive aggressive treatment because some low-risk tumours may not have caused harm.[7] Furthermore, overtreatment of PCa has the potential to result in urine incontinence and erectile dysfunction, among other things.[8]

According to the European Association of Urology-European Association of Nuclear Medicine-European Society for Radiotherapy and Oncology-European Society of Urogenital Radiology-International Society of Geriatric

Oncology (EAU-EANM-ESTRO-ESUR-SIOG) and The National Comprehensive Cancer Network (NCCN) guidelines,[9,10] PCa is categorised into three risk groups: low risk, intermediate risk, and high risk. Low-risk PCa is eligible for active surveillance (AS), with the majority of patients not experiencing symptomatic progression during their lifespan.[9–11] For intermediate- and high-risk PCa, surgery and radiation remain widely used.[9,10,12] Nevertheless, there is still a debate about whether AS protocols can be extended to patients who have intermediate-risk PCa with a greater risk of metastasis.[11] As a result, the proper risk classification of PCa can greatly benefit clinical decision-making and outcomes. Current guidelines for the risk stratification of PCa rely primarily on PSA level, Gleason score (GS) and T stage, particularly with pathologic GS, which is generally believed to be a critical prognostic predictor. Pathologic tissues obtained for GS assessment by prostate biopsy can undoubtedly give relatively accurate results, but this process also has potential adverse complications, such as haemorrhage and urinary tract infections (UTIs). As a result, a non-invasive and predictable tool available for accurate risk stratification is needed to help customize treatment and surveillance strategies.

Radiomics[13] and machine learning (ML) have been proven to be promising tools in the development of quantitative biomarkers for medical imaging. Tools such as radiomics and ML, an artificial intelligence subfield, may actually improve risk stratification. Radiomic features can potentially decode medical images to completely and non-invasively capture tumour phenotypic characteristics quantitatively and have demonstrated favourable predictive results for PCa detection,[14,15] tumour invasiveness,[16–18] and post-operative management.[19,20] ML has also been proposed for a wide range of applications in medical imaging and can utilise radiomic features to automatically infer decisions from data sets with the purpose of developing a decision-making model, such as models for the detection and characterisation of neoplastic lesions.[21,22] Previous works have explored radiomics, ML and deep learning algorithms for cancer stratification, such as endometrial cancer,[23] indeterminate pulmonary nodules[24] and PCa. In the instance of PCa, Sarah O.S. Osman et al clarified the role of CT-based radiomic features in PCa risk stratification.[25] Bino Varghese et al developed an ML classifier for the pre-operative prediction of low/intermediate- and high-risk PCa based on multiparametric MRI (mpMRI)-based radiomic features.[26] However, there is still a paucity of studies on accurate risk stratification based on ML, notably independent analysis in the intermediate-risk category, which would achieve more precise and tailored patient therapy. Highly accurate and reliable ML methods are expected to drive the success of radiomics applications, which will be useful at diagnosis, particularly in guiding AS protocols and upstaging criteria for tailored disease management.

The inclusion of MRI-based radiomics in ML models may provide a more complete picture of PCa risk stratification, leading to novel insights. However, to our knowledge, few studies have investigated PCa risk stratification from an ML perspective. We innovatively analysed the intermediate-risk group as an individual in an ML model and compared the performance of different ML models and traditional marker (the mean ADC value) in predicting the PCa risk extent to achieve more effective and personalised patient therapies.

METHODS AND MATERIALS

The general framework of this study is depicted in Figure 1. This retrospective study was approved by the institutional review board, and the requirement to obtain written informed consent was waived. The study was performed in accordance with the Declaration of Helsinki (as revised in 2013).

Patients

A total of 229 consecutive patients with histologically proven PCa underwent MRI screening between August 2016 and May 2021 in the hospital, and 213 PCa patients were recruited in this study according to the following inclusion criteria and exclusion criteria. The inclusion criteria were as follows: (1) complete clinical data; (2) pathological results of suspicious prostate lesions acquired by biopsy or prostatectomy; and (3) no prior prostate surgery, biopsy, radiation therapy, or endocrine therapy before

Figure 1. Flow diagram of the ML workflow. ML, machine learning.

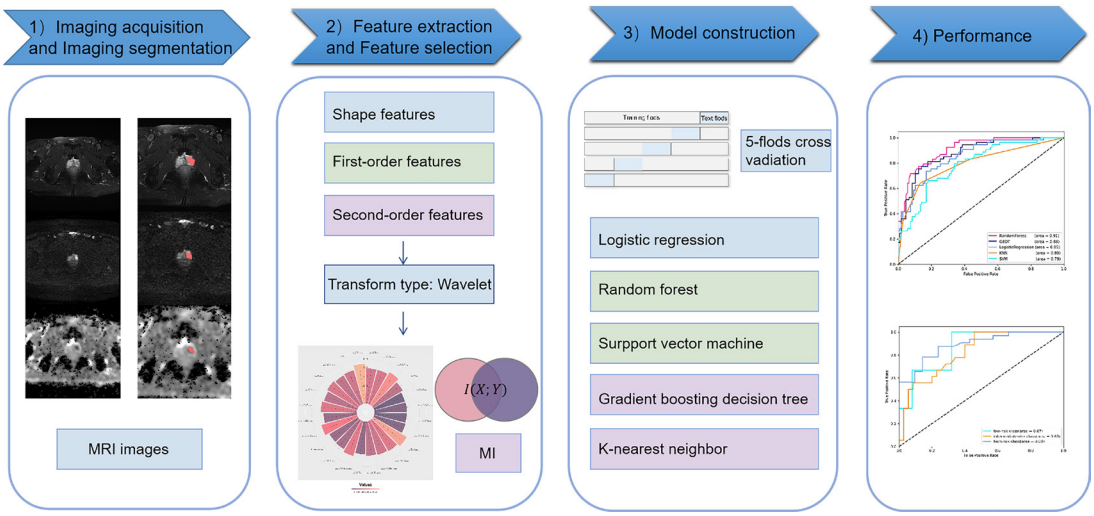

Figure 2. Flowchart of patient selection. PCa, prostate cancer.

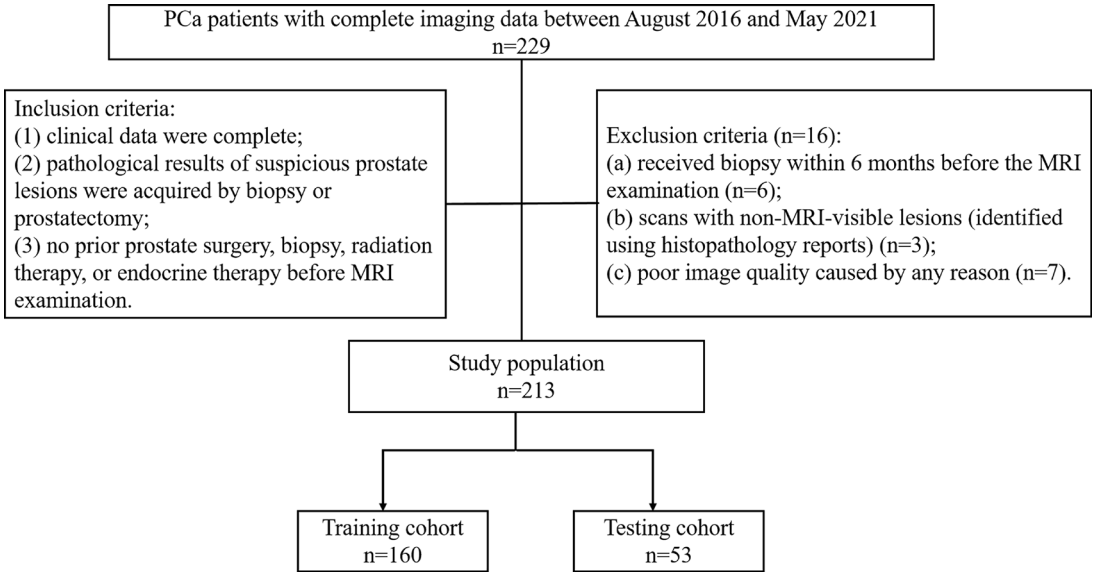

MRI examination. The exclusion criteria were as follows: (a) received biopsy within 6 months before the MRI examination; (b) scans with non-MRI-visible lesions (identified using histopathology reports); and (c) poor image quality caused by any reason. The final study population and details of patient selection are shown in Figure 2.

MRI examination parameters

A 3.0 T MRI scanner was used (MAGNETON Prisma; SIEMENS A Tim + Dot System), and an 8-channel phased array software coil was used to collect MR images. The prostate, seminal vesicles, and as many adjacent structures as possible were scanned. The parameters for axial fat suppression (FS) T_2 weighted imaging (T_2WI) were as follows: repetition time (TR): 3090 ms; echo time (TE): 77 ms; layer thickness: 3 mm; averages: 2; field of vision (FOV): 20 × 20 cm; and acquisition matrix: 320 × 240. Diffusion-weighted imaging (DWI) was performed on the axial plane, with the same azimuth and position as axial FS T_2 weighted MRI, and obtained by an axial EPI sequence: TR: 3800 ms; TE: 84 ms; layer thickness: 3 mm; NEX: 2; FOV: 20 × 20 cm; acquisition matrix: 118 × 118; and b values: 1400 s/mm2. Apparent diffusion coefficient (ADC) maps were calculated on a designated workstation (Advanced Workstation 4.6; GE Medical Systems, Milwaukee, Wisconsin; FUNCTOOL).

Risk stratification assessment

According to the classification proposed by the EAU-EANM-ESTRO-ESUR-SIOG,[9] based on PSA, GS and T stage, the patients were stratified into three risk groups (low-risk, intermediate-risk and high-risk groups). The details of the classification standard are shown in Table 1. First, the PSA threshold values chosen for laboratory indicators were based on the normal ranges used at our institution. Second, the biopsy procedure was performed by an experienced urologist, and the specimen was assessed by a pathologist. In the pathological results, the GS (describing the largest and a secondary area of the tumour) of all prostate samples was included. Third, one urologist with 10 years of experience ascertained the T stage based on the staging system proposed by the American Joint Committee on Cancer/Union for International Cancer Control (AJCC/UICC).[27] Finally, the risk stratification of PCa was appraised by a urologist with 20 years of experience.

Image segmentation

All pre-operative MRI images, including T_2WI, DWI (The averaged DWI signal from three directions) and ADC images, were imported into Artificial Intelligence Kit software (A.K. software; GE Healthcare, China) to delineate the region of interest (ROI) of tumour areas. ROIs were delineated separately and connected as a whole when dealing with multifocal prostate cancer. The ADC maps were imported into syngo.via (Siemens Healthcare GmbH, 2020, Erlangen, Germany) , the ADC value was automatically calculated after the ROIs was delimited, then the regional mean ADC values were calculated. All these ROIs were manually delineated slice by slice and each plane was superimposed by two radiologists with more than 10 years of experience in

Table 1. Patient grouping was based on the EAU-EANM-ESTRO-ESUR-SIOG guidelines

Risk group	Low risk	Intermediate risk	High risk	
Definition	PSA<10 ng ml^{-1}, ISUP Grade 1 (GS<7) and cT1-2a	PSA 10–20 ng ml^{-1}, ISUP Grade 2/3 (GS = 7) or cT2b	PSA>20 ng ml^{-1}, ISUP Grade 4/5 (GS>7) or cT2c	Any PSA, any GS (any ISUP grade), cT3–4, or cN+

EAU-EANM-ESTRO-ESUR-SIOG, European Association of Urology-European Association of Nuclear Medicine-European Society for Radiotherapy and Oncology-European Society of Urogenital Radiology-International Society of Geriatric Oncology; GS = Gleason score; ISUP = International Society for Urological Pathology; PSA = prostate-specific antigen.

clinical diagnosis to ensure the reproducibility of the intra- and interobserver segmentation. All divergences were discussed until a consensus was reached.

Radiomic feature extraction

With Artificial Intelligence Kit software, the quantitative features of the ROIs were calculated, and a total of 107 radiomic features were extracted by each MRI parameter, including 14 shape features, 18 first-order features, and 75 second-order features. These features included the grey level co-occurrence matrix, grey level run-length matrix, grey level size zone matrix, grey level dependence matrix, and neighbouring grey tone difference matrix. These features were then wavelet transformed to generate 851 radiomic features. Therefore, a total of 2553 radiomic features were extracted from T_2WI, DWI and ADC sequences.

Radiomic feature selection and model building

First, the radiomic features extracted from the ROIs of each MRI sequence were normalised separately using the Z score. Second, to reduce irrelevant features, mutual information (MI) was adopted, which measures the stochastic dependence of discrete variables.[28] The formula was as follows:

$$I(X;Y) = \sum_{x \in X} \sum_{y \in Y} P(x,y) \log \frac{P(x,y)}{P(x)P(y)}$$

where X is the selected radiomic feature, and Y is the respective coefficient of radiomic feature determined by MI. Via the mutual information algorithm, each feature has its quantitative absolute value, then using min-max normalisation, the values below the 80% threshold are discarded. Finally, based on the selected radiomic features, five ML approaches were used to generate predictive models. These approaches included logistic regression (LR), random forest (RF), k-nearest neighbour (KNN), gradient boosting decision tree (GBDT) and support vector machine (SVM). To lower the impact of imbalanced samples, the synthetic minority oversampling technique (SMOTE) method was adopted,[29] which generated a sample from the joint weighting of multiparametric features. The subjects were randomly divided into two subsets, 80% for model training and 20% for validation. A fivefold cross-validation approach was applied to validate the performance of the ML models.

Statistical analysis

Python codes and IBM SPSS 25.0 (IBM corporation, NEW York) for Windows were employed for these analyses, including feature selection, classification and statistical analyses. The MI feature selection algorithm was used to identify and rank the order of the top 24 radiomic features that differentiate different risk groups within the training set. Continuous variables were analysed through one-way ANOVA and are expressed as the mean ± standard deviation (SD). A p value <0.05 was considered statistically significant. The trained classifiers were validated using the testing set and assessed in terms of the area under the receiver operating characteristic curve (AUC). Multilesion cases were constrained to only be within one subset (all lesions from a single patient were strictly used for either training or validation but never for both).

RESULTS

Patient characteristics

After considering the inclusion and exclusion criteria, a total of 213 patients were enrolled in the study. There were 16 low-risk (average age 71.00 ± 9.19 years), 65 intermediate-risk (average age 73.22 ± 7.49 years), and 132 high-risk (average age 72.38 ± 8.20 years) PCa patients based on the overall findings. No significant difference in age was observed among the three groups ($F = 0.617$, $p > 0.05$).

Selected features

After sufficient dimension reduction, 24 radiomic features were selected and listed in order of importance by the MI algorithm. These 24 radiomic features consisted of 19 second-order features and 5 first-order statistics, with 13 from DWI, 9 from T_2WI, and only 2 from ADC. Of these, the T_2WI radiomic feature (wavelet-LLL NGTDM Coarseness) had the best correlation with risk stratification. More details about the selected radiomic features are shown in Figure 3.

The overall classification performance of different ML models

The AUC values of the five models were all higher than 0.6 (range from 0.65 to 0.87), which indicates that the selected radiomic features have good reliability. The five ML algorithms demonstrated various accuracies in identifying the risk of PCa. Of these five classifiers, the RF model predicted the overall risk stratification of PCa the best (AUC = 0.87), followed by the GBDT model (AUC = 0.85) and then the LR model (AUC = 0.75). The RF model outperformed the traditional marker like the mean ADC value (AUC = 0.82). In addition, the accuracy, precision and recall of the RF model were 0.79, 0.78 and 0.79, respectively, which were higher than those of the other algorithms in model evaluation, indicating that this model has a good classification ability. A comparison of ROC curves for the five ML models and the mean ADC value is displayed in Figure 4, while the accuracy, precision and recall of all the algorithms are presented in Table 2.

Subgroup classification performance based on the RF method

Further analysis based on the RF model showed that it had excellent predictive performance in each subgroup (range 0.83–0.89), as shown in Figure 5. For the high-risk group, the AUC was 0.89. The precision, recall, F1-score and sensitivity of the high risk group were 0.81, 0.94, 0.87 and 0.94, respectively. The model had higher specificity in the low- and intermediate-risk groups than in the high-risk group and achieved a specificity of 0.90 and above. The classification performance outcomes of the RF classifier in the test set are summarised in Table 3.

DISCUSSION

We established a three-class ML model with satisfactory performance for PCa patient risk stratification based on radiomic features. The results showed that the RF algorithm had the best performance compared to the other algorithms in predicting PCa risk stratification. In addition, the AUCs of the RF model for the three risk groups were significantly higher than 0.8, supporting the excellent prediction ability of this model. Radiomics-based

Figure 3. Radiomic features selected by the MI algorithm. Note: Via the mutual information algorithm, each feature has its quantitative absolute value and then using min-max normalisation. A ranking criterion to remove features below the threshold (0.8). This figure shows its origin absolute value. DWI, diffusion-weighted imaging; MI, mutual information

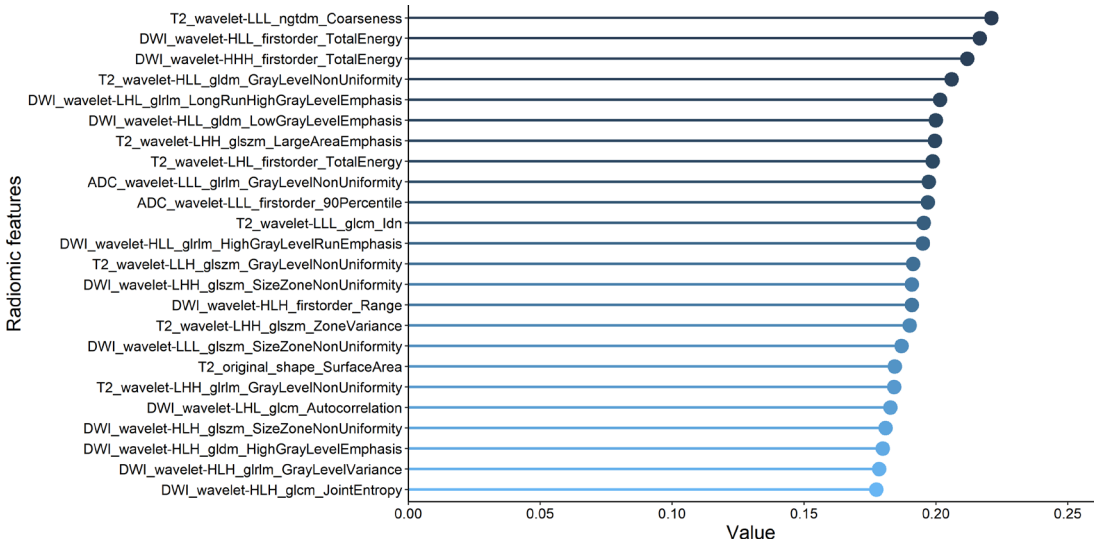

ML models provide a better tool for risk classification, which helps to further reduce both overdiagnosis and overtreatment as well as provide personalised treatments.

In the present study, 24 meaningful radiomic features were identified. Only one feature was from the original image, the rest of the features were after wavelet transform. The wavelet transform contains the full information of the original signal from the point of information processing, has the ability to provide high time resolution in high frequency which provided a precise and unifying frame work for the analysis and characterisation of a signal at different scales,[30] consisting of 19 second-order features and 5 first-order statistical features, of which 13 were from DWI, 9 were from T_2WI, and only 2 were from ADC. Varghese et al found that second-order features play a crucial role in the risk classification of patients with PCa.[26] This was consistent with the finding of our study; second-order features quantify the complex variations of every adjacency voxel's signal intensity distribution with spatial grey level dependence matrices, potentially reflecting inherently aggressive tumour biology.[31] Furthermore, our study included shape features which provided much information to predict risk classification, such as sphericity and surface area. Ahmadet et al discovered that intratumoral radiomic features on biparametric MRI accurately stratified PCa risk, and the radiomic features were mainly derived from first-order statistics of ADC sequences and based on Gabor and Haralick.[32] In contrast, radiomic features from DWI and T_2WI sequences were top ranked in this study. We speculate that the difference may be related to different grouping methods. Intermediate- and high-risk groups were combined in Ahmadet et al's research (low- *vs* high-risk and low- *vs* intermediate- and high-risk). The differences between the low-risk group and others are mainly due to tumour heterogeneity, which is mainly reflected by DWI and ADC sequences. When the intermediate-risk group was listed separately, the complexity of influencing factors was increased, especially the influence of T stage. The size of the tumour and its

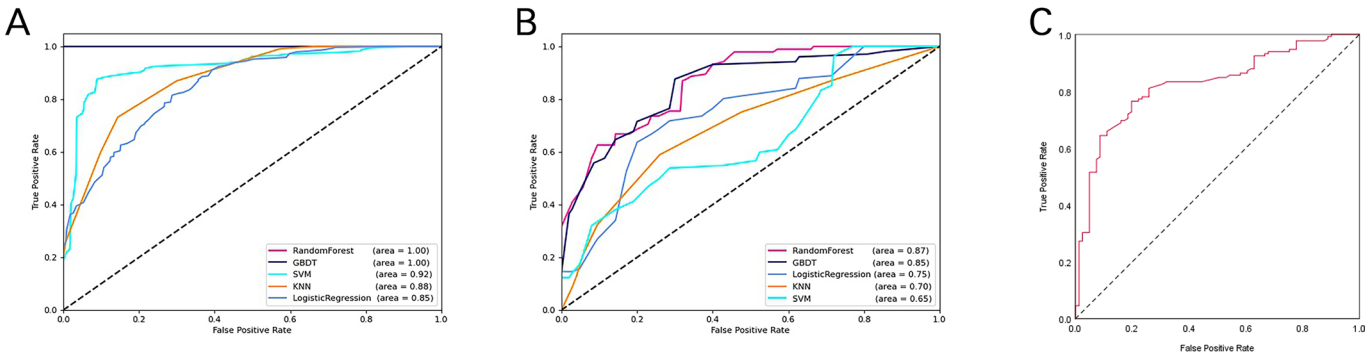

Figure 4. ROC curves of the five ML models and the mean ADC value to assess the overall performance of PCa risk prediction. Note: (A, B) The ROC curves of the five radiomics models in the training cohort and the text cohort. The five ML models include LR, RF, GBDT, KNN and SVM. (C) The performance of traditional marker (the mean ADC value) in stratifying PCa risks. ADC, apparent diffusion coefficient; GBDT, gradient boosting decision tree; KNN, k-nearest neighbour; LR, logistic regression; ML, machine learning; PCa, prostate cancer; ROC, receiver operating characteristic curve; RF, random forest; SVM, support vector machine.

Table 2. Performance of five different ML models in predicting PCa risk stratification

Classifier	AUC	Accuracy	Precision	Recall
LR	0.75	0.70	0.69	0.70
RF	0.87	0.79	0.78	0.79
GBDT	0.85	0.75	0.76	0.75
SVM	0.65	0.62	0.65	0.62
KNN	0.70	0.66	0.70	0.66

Note: The five ML models include LR, RF, GBDT, KNN and SVM.
AUC, area under the curve; GBDT, gradient boosting decision tree; KNN, k-nearest neighbour; LR, logistic regression; ML, machine learning; PCa, prostate cancer; ROC, receiver operating characteristic curve; RF, random forest; SVM, support vector machine.

invasion border were assessed by T stage, and T_2WI was found to be more accurate in depicting the zonal description of the lesion anatomy and its surroundings than DWI and ADC. Therefore, we consider that DWI features reflecting tumour heterogeneity and T_2WI features representing tumour boundaries both play a key role in this three-class ML model.

With the increasing interest in AI algorithms and relevant applications in PCa, we were inspired to explore the possibility of ML in risk classification to assist in decision-making and benefit patients. Five ML models were established, including RF, LR, GBDT, SVM and KNN models; among these models, the prediction performance of the GBDT and RF models was outstanding. RF and GBDT are both ensemble learning techniques,[33] a methodology that combines multiple individual learners, which improves the generalisation performance of the classification algorithm. BinoVarghese et al identified the best performing classifier for PCa risk stratification based on mpMRI-derived radiomic features, and the quadratic kernel-based SVM (QSVM)[26] classifier achieved the highest overall absolute performance. The reason why QSVM showed such effectiveness can be partly attributed to the use of kernels (square of the dot product in this case) that can represent the non-Euclidean similarity or distance between data points without having to transform the points into non-Euclidean spaces.[34] The high performance of the RF, GBDT, and SVM classifiers suggests that it is vital to utilise sufficiently flexible ML techniques to incorporate the nonlinear relationships between characteristics and risk extent when using radiomics for PCa risk stratification. More recently, contradictory findings have revealed that there are no unified ML

Figure 5. ROC curve for the performance of the RF model in different risk classes. ROC, receiver operating characteristic curve; RF, random forest.

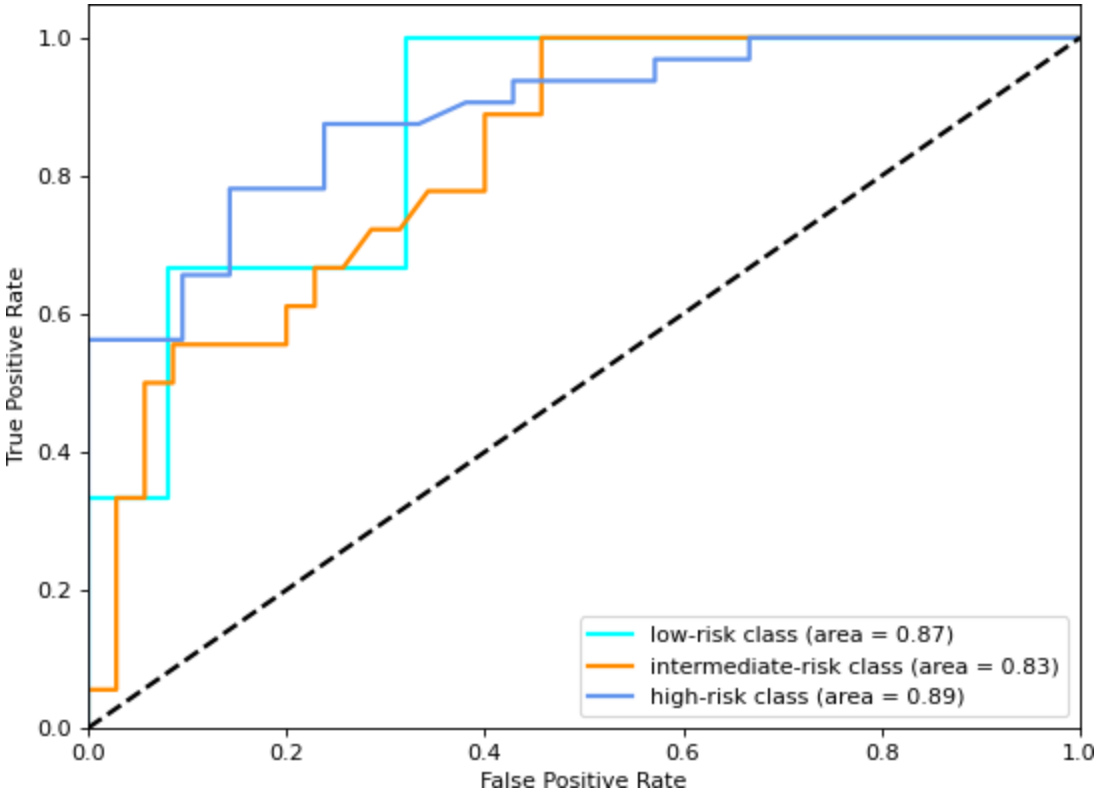

Table 3. Performance outcomes of the RF model in different risk groups

Risk group	Precision	Recall	F1-score	Sensitivity	Specificity
Low-risk	0.50	0.33	0.40	0.33	0.98
Intermediate-risk	0.79	0.61	0.69	0.61	0.91
High-risk	0.81	0.94	0.87	0.94	0.67

RF, random forest.

algorithms in radiomics.[35] A systematic and rigorous ML framework comprises feature selection, classification, cross-validation, algorithm selection and statistical analyses. Variations in these steps will affect the efficiency of the model to some degree, and the various algorithms showed both advantages and disadvantages. When the data are unbalanced, it is crucial to combine the nonlinear relationship between features and research objectives; nevertheless, the larger the sample is, the smaller the influence of algorithm selection. Therefore, to achieve a higher accuracy of classification, a variety of feature selection methods, data balancing methods, and ML algorithms should be used, and after cross-validation, the best performing models are developed.

This study also had some limitations that should be noted. First, the ROIs of PCa were manually delineated by two radiologists in our study and could be semi-automatically or automatically segmented in future studies. Second, all pathological results were biopsy-proven and lacked further validation with radical prostatectomy specimens. Third, for patients with multifocal lesions, we did not have biopsy confirmation of every multifocal lesion, only a per-patient level categorisation of high-, intermediate- or low-risk disease was made. Fourth, the value of the comparison between single- and multiple-sequence in classifying prostate risk stratification needs to be further studied. Last, because this was a single-centre retrospective study, the performance of the RF algorithm should be further validated in multicentre studies.

Despite these limitations, the current study is proof of concept that the RF model showed great performance and can exactly characterise the risk stratification of PCa. The proposed image-based approach provides an alternative method for non-invasive risk stratification, which can benefit tailored therapeutic schedules and reduce the suffering of patients with PCa. External validation and prospective studies are warranted to verify our findings.

ACKNOWLEDGEMENTS

This work was supported by the General Program of Chongqing Natural Science Foundation (cstc2019jcyj-msxmX0073), Joint project of Chongqing Health Commission and Science and Technology Bureau (2019GDRC011), the National Major Science and Technology Projects of China (2018AAA0100703), High-Level Medical Reserved Personnel Training Project of Chongqing and Kuanren Talents Program of the Second Affiliated Hospital of Chongqing Medical University. The authors would like to thank Xilin Gu, Yuanfeng Zhang and Chuan Liu for reviewing and assessing the cases. All authors reviewed the manuscript.

CONFLICTS OF INTERESTS

None of the authors have any conflicts of interest to disclose.

REFERENCES

1. Key Statistics for Prostate Cancer | Prostate Cancer Facts. Available from: https://www.cancer.org/cancer/prostate-cancer/about/key-statistics.html (accessed 20 Jun 2018)
2. Siegel RL, Miller KD, Fuchs HE, Jemal A. Cancer statistics, 2021. *CA Cancer J Clin* 2021; **71**: 7–33. https://doi.org/10.3322/caac.21654
3. Schröder FH, Hugosson J, Roobol MJ, Tammela TLJ, Ciatto S, Nelen V, et al. Screening and prostate-cancer mortality in a randomized European study. *N Engl J Med* 2009; **360**: 1320–28. https://doi.org/10.1056/NEJMoa0810084
4. Hugosson J, Carlsson S, Aus G, Bergdahl S, Khatami A, Lodding P, et al. Mortality results from the Göteborg randomised population-based prostate-cancer screening trial. *Lancet Oncol* 2010; **11**: 725–32. https://doi.org/10.1016/S1470-2045(10)70146-7
5. Kilpeläinen TP, Tammela TLJ, Roobol M, Hugosson J, Ciatto S, Nelen V, et al. False-Positive screening results in the European randomized study of screening for prostate cancer. *Eur J Cancer* 2011; **47**: 2698–2705. https://doi.org/10.1016/j.ejca.2011.06.055
6. Grossman DC, Curry SJ, et al, US Preventive Services Task Force. Screening for prostate cancer: U.S. preventive services task force recommendation statement. *JAMA* 2018; **319**: 1901–13.
7. Loeb S, Bjurlin MA, Nicholson J, Tammela TL, Penson DF, Carter HB, et al. Overdiagnosis and overtreatment of prostate cancer. *Eur Urol* 2014; **65**: 1046–55. https://doi.org/10.1016/j.eururo.2013.12.062
8. Bangma CH , Roemeling S , Schrder FH . Overdiagnosis and overtreatment of early detected prostate cancer. World J Urol. 2007; 25(1):3-9.
9. Mottet N, Bellmunt J, Bolla M, Briers E, Cumberbatch MG, De Santis M, et al. EAU-ESTRO-SIOG guidelines on prostate cancer. Part 1: screening, diagnosis, and local treatment with curative intent. *European Urology* 2017; **71**: 618–29. https://doi.org/10.1016/j.eururo.2016.08.003
10. (N.d.). National comprehensive cancer network. NCCN clinical practice guidelines in oncology. *Prostate Cancer Version 12021 Available from:Https://WwwNccnOrg/Patients/Guidelines/Prostate/Files/Assets/Basichtml/Page-1Html#.*
11. Popiolek M, Rider JR, Andrén O, Andersson S-O, Holmberg L, Adami H-O, et al. Natural history of early, localized prostate cancer: a final report from three decades of follow-up.

Eur Urol 2013; **63**: S0302-2838(12)01221-3: 428–35: . https://doi.org/10.1016/j.eururo.2012.10.002
12. Spence W. Personalising prostate radiotherapy in the era of precision medicine: a review. *J Med Imaging Radiat Sci* 2018; **49**: S1939-8654(17)30238-2: 376–82: . https://doi.org/10.1016/j.jmir.2018.01.002
13. Lambin P, Leijenaar RTH, Deist TM, Peerlings J, de Jong EEC, van Timmeren J, et al. Radiomics: the bridge between medical imaging and personalized medicine. *Nat Rev Clin Oncol* 2017; **14**: 749–62. https://doi.org/10.1038/nrclinonc.2017.141
14. Cameron A, Khalvati F, Haider MA, et al. MAPS: A Quantitative Radiomics Approach for Prostate Cancer Detection.IEEE Trans Biomed Eng.2016;63:1145-1156.
15. Wang J, Wu C-J, Bao M-L, Zhang J, Wang X-N, Zhang Y-D. Machine learning-based analysis of Mr radiomics can help to improve the diagnostic performance of PI-RADS V2 in clinically relevant prostate cancer. *Eur Radiol* 2017; **27**: 4082–90. https://doi.org/10.1007/s00330-017-4800-5
16. Chen T, Li M, Gu Y, Zhang Y, Yang S, Wei C, et al. Prostate cancer differentiation and aggressiveness: assessment with a radiomic-based model vs. pi-rads V2. *J Magn Reson Imaging* 2019; **49**: 875–84. https://doi.org/10.1002/jmri.26243
17. Ma S, Xie H, Wang H, Yang J, Han C, Wang X, et al. Preoperative prediction of extracapsular extension: radiomics signature based on magnetic resonance imaging to stage prostate cancer. *Mol Imaging Biol* 2020; **22**: 711–21. https://doi.org/10.1007/s11307-019-01405-7
18. Losnegård A, Reisæter LAR, Halvorsen OJ, Jurek J, Assmus J, Arnes JB, et al. Magnetic resonance radiomics for prediction of extraprostatic extension in non-favorable intermediate- and high-risk prostate cancer patients. *Acta Radiol* 2020; **61**: 1570–79. https://doi.org/10.1177/0284185120905066
19. Bourbonne V, Vallières M, Lucia F, Doucet L, Visvikis D, Tissot V, et al. MRI-derived radiomics to guide post-operative management for high-risk prostate cancer. *Front Oncol* 2019; **9**: 807: 807: . https://doi.org/10.3389/fonc.2019.00807
20. Zhong Q-Z, Long L-H, Liu A, Li C-M, Xiu X, Hou X-Y, et al. Radiomics of multiparametric MRI to predict biochemical recurrence of localized prostate cancer after radiation therapy. *Front Oncol* 2020; **10**: 731: 731: . https://doi.org/10.3389/fonc.2020.00731
21. Naz J, Sharif M, Yasmin M, Raza M, Khan MA. Detection and classification of gastrointestinal diseases using machine learning. *Curr Med Imaging* 2021; **17**: 479–90. https://doi.org/10.2174/1573405616666200928144626
22. Cuocolo R, Cipullo MB, Stanzione A, Ugga L, Romeo V, Radice L, et al. Machine learning applications in prostate cancer magnetic resonance imaging. *Eur Radiol Exp* 2019; **3**(1): 35. https://doi.org/10.1186/s41747-019-0109-2
23. Chen J, Gu H, Fan W, Wang Y, Chen S, Chen X, et al. Mri-Based radiomic model for preoperative risk stratification in stage I endometrial cancer. *J Cancer* 2021; **12**: 726–34. https://doi.org/10.7150/jca.50872
24. Massion PP, Antic S, Ather S, Arteta C, Brabec J, Chen H, et al. Assessing the accuracy of a deep learning method to risk stratify indeterminate pulmonary nodules. *Am J Respir Crit Care Med* 2020; **202**: 241–49. https://doi.org/10.1164/rccm.201903-0505OC
25. Osman SOS, Leijenaar RTH, Cole AJ, Lyons CA, Hounsell AR, Prise KM, et al. Computed tomography-based radiomics for risk stratification in prostate cancer. *Int J Radiat Oncol Biol Phys* 2019; **105**: S0360-3016(19)33392-9: 448–56: . https://doi.org/10.1016/j.ijrobp.2019.06.2504
26. Varghese B, Chen F, Hwang D, Palmer SL, De Castro Abreu AL, Ukimura O, et al. Objective risk stratification of prostate cancer using machine learning and radiomics applied to multiparametric magnetic resonance images. *Sci Rep* 2019; **9**(1). https://doi.org/10.1038/s41598-018-38381-x
27. Bhindi B, Karnes RJ, Rangel LJ, Mason RJ, Gettman MT, Frank I, et al. Independent validation of the American joint Committee on cancer 8th edition prostate cancer staging classification. *Journal of Urology* 2017; **198**: 1286–94. https://doi.org/10.1016/j.juro.2017.06.085
28. Zaffalon M, Hutter M. Robust Feature Selection by Mutual Information Distributions. UAI 2002;14:577-584.
29. Chawla NV, Bowyer KW, Hall LO, Kegelmeyer WP. SMOTE: synthetic minority over-sampling technique. *Jair* 2002; **16**: 321–57. https://doi.org/10.1613/jair.953
30. Wang TC, Karayiannis NB. Detection of microcalcifications in digital mammograms using wavelets. *IEEE Trans Med Imaging* 1998; **17**: 498–509. https://doi.org/10.1109/42.730395
31. Davnall F, Yip CSP, Ljungqvist G, Selmi M, Ng F, Sanghera B, et al. Assessment of tumor heterogeneity: an emerging imaging tool for clinical practice? *Insights Imaging* 2012; **3**: 573–89. https://doi.org/10.1007/s13244-012-0196-6
32. Algohary A, Shiradkar R, Pahwa S, Purysko A, Verma S, Moses D, et al. Combination of peri-tumoral and intra-tumoral radiomic features on bi-parametric MRI accurately stratifies prostate cancer risk: a multi-site study. *Cancers (Basel)* 2020; **12**(8): 2200. https://doi.org/10.3390/cancers12082200
33. Webb GI, Zheng Z. Multistrategy ensemble learning: reducing error by combining ensemble learning techniques. *IEEE Trans Knowl Data Eng* 2004; **16**: 980–91. https://doi.org/10.1109/TKDE.2004.29
34. Burges CJC. A tutorial on support vector machines for pattern recognition. *Data Mining and Knowledge Discovery* 1998; **2**: 121–67. https://doi.org/10.1023/A:1009715923555
35. Parmar C, Grossmann P, Bussink J, Lambin P, Aerts H. Machine learning methods for quantitative radiomic biomarkers. *Sci Rep* 2015; **5**: 13087. https://doi.org/10.1038/srep13087